Inelastic scattering from local vibrational modes

Balázs Dóra* and Miklós Gulácsi
Max-Planck-Institut für Physik Komplexer Systeme, Nöthnitzer Strasse 38, 01187 Dresden, Germany
(Received 12 September 2008; published 13 October 2008)

We study a nonuniversal contribution to the dephasing rate of conduction electrons due to local vibrational modes. The inelastic-scattering rate is strongly influenced by multiphonon excitations, exhibiting oscillatory behavior. For higher frequencies, it saturates to a finite, coupling dependent value. In the strong-coupling limit, the phonon is almost completely softened and the inelastic cross section reaches its maximal value. This represents a magnetic-field insensitive contribution to the dephasing time in mesoscopic systems, in addition to magnetic impurities.

DOI: 10.1103/PhysRevB.78.165111 PACS number(s): 73.23.−b, 72.10.Fk, 73.63.−b

The loss of quantum coherence, occurring through inelastic processes during which some excitations are left behind and the outgoing state is not a single-particle state anymore, is characterized by the dephasing time, τ_ϕ. The dephasing time can reliably be estimated from the low-field magnetoresistance data from the weak-localization corrections to the Drude conductivity.[1] In general, any dynamical impurity with internal degrees of freedom can dephase conduction electrons. If the impurity changes its state, the environment felt by the electrons changes, causing dephasing.

Recently, dephasing due to magnetic impurities has been addressed successfully in the relevant temperature range (around and below the Kondo temperature[2]) by relating the dephasing time to the inelastic cross section.[3–7] The latter can be determined from the knowledge of the many-body T matrix. It accounts nicely for various features of the dephasing time such as its saturation above the Kondo temperature. However, in many systems, Coulomb-type interaction is not the only source of correlation, which leads us to consider the interaction of electrons with local vibrational (phononic) modes.[8] The interest to study this model is at least threefold: first, artificial quantum dots based on single molecules[9] (e.g., C_{60}) usually distort upon the addition or removal of electrons and can act as a quantized nanomechanical oscillator by single electron charging.[9] Moreover, other realization contains suspended quantum dot cavity,[10] where confined phonon modes influence the transport. Second, in many strongly correlated systems, such as heavy fermions or valence fluctuation systems, lattice vibrations are known to couple strongly to electrons. The recent discovery of magnetically robust heavy fermion behavior in filled skutterudite compound[11] $SmOs_4Sb_{12}$ renewed interest in Kondo phenomena with phononic origin.[12,13] Both the specific-heat coefficient and coefficient of the quadratic temperature dependence of the electrical resistivity were found to be almost independent of an applied magnetic field.

Finally, yet another motivation arises from recent experiments on $Cu_{93}Ge_4Au_3$ thin films,[14] where the observed dephasing time was found to be rather insensitive to high magnetic fields, suggesting nonmagnetic dephasing processes, such as dynamical defects.

Therefore, it is timely to investigate other sources of dephasing beside magnetic impurities, such as a localized oscillator.[8] In general, these dynamic point defects are randomly distributed in a system. By assuming that the impurities are distributed sufficiently far from each other, it suffices to study one single mode with fixed energy ω_0 (Einstein oscillator), similarly to the treatment of magnetic impurities.[2] The phonon can couple to the local charge density and modify the local potential felt by the electron (single impurity Holstein model[15–17]). In the most general case, this amounts to the study of the Yu-Anderson or single impurity Holstein model (visualized in Fig. 1) given by[18–20]

$$H = \sum_k \varepsilon(k) c_k^+ c_k + g_d Q \Psi^+(0)\Psi(0) + \frac{P^2}{2m} + \frac{m\omega_0^2}{2} Q^2, \quad (1)$$

which describes three-dimensional (3D) electrons interacting with a local bosonic mode, $\Psi(\mathbf{r})$ denotes the bulk 3D electron field operator, and c_k its Fourier components. This accounts for intrinsic and extrinsic point defects such as interstitial or substitutional impurities.[21] From the latter class, foreign atoms [such as Fe in Ag or Au (Refs. 1 and 7)] mainly represent a source of potential scattering. Beyond this, they are capable of magnetic scattering[5,6] and can cause a modification of the local phononic environment as well, resulting in a Hamiltonian such as Eq. (1). Besides foreign atoms, the self-interstitial impurities (proper atom at a nonlattice site) also distort the local potential background felt by the conduction electrons, leading to local electron–phonon interaction. This model has a rich history in the field of nonlinear impurities.[22] In quantum optics, such model arises in arrays of nonlinear optical waveguides for example. Moreover, in the condensed-matter context, Eq. (1) bears close resemblance to the Anderson-Holstein impurity model,[23,24]

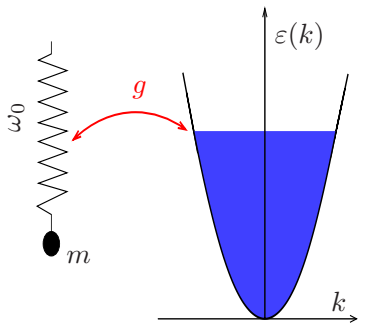

FIG. 1. (Color online) Schematic of a nanomechanical resonator coupled to a conduction-electron bath.

describing molecular vibrations in quantum dots. It can be regarded as a generalization of scattering on two-level systems to the multilevel case.[25,26]

Due to the isotropic nature of the electron–phonon coupling, the electron field operators can be expanded in the appropriate angular-momentum channels (depending on the dimensionality of the conduction electrons), and only the s-wave component couples to the impurity[27] as

$$\Psi(\mathbf{r}) = \frac{e^{ik_F r}R(r) - e^{-ik_F r}R(-r)}{2i\sqrt{\pi}r} + \frac{\text{higher}}{\text{harmonics}}, \tag{2}$$

where $R(x)$ stands for the chiral, right moving radial component, $r \geq 0$ is the radial coordinate in the original 3D system, and k_F is the Fermi wave number. Here, instead of a right $[R(r)]$ and left $[L(r)]$ moving field on a half line, we introduced a single chiral field on the whole line $(-\infty < x < \infty)$ with $L(r)=R(-r)$, as is customary.[27] Thus, the model can be mapped onto an effective model of chiral fermions, interacting with the bosonic mode at the origin:

$$H = -iv\int_{-\infty}^{\infty} dx R^+(x)\partial_x R(x) + gQ\rho(0) + \frac{P^2}{2m} + \frac{m\omega_0^2}{2}Q^2, \tag{3}$$

and only the radial motion of the particles is accounted for by chiral (right moving) fermion field, $\rho(x) =: R^+(x)R(x)$: is the normal ordered electron charge density, v is the Fermi velocity, $g = g_d k_F^2/\pi$ describes the local electron–phonon coupling, m and ω_0 are the phononic mass and frequency, respectively, and Q and P are the phonon displacement field and momentum conjugate to it. In the spirit of the Yu-Anderson model,[19] the phonons couple to the electronic density fluctuations in our model as well. The ground state will be degenerate, similarly to the Kondo problem,[2] between occupied and unoccupied electron states, leading to the formation of a double-well potential.[19] Upon bosonization,

$$R(x) = \frac{1}{\sqrt{2\pi\alpha}}\exp[i\sqrt{4\pi}\Phi(x)], \tag{4}$$

with $[\Phi(x),\Phi(y)] = i\,\mathrm{sgn}(x-y)/4$, the Hamiltonian reads as

$$H = v\int_{-\infty}^{\infty} dx[\partial_x\Phi(x)]^2 + \frac{g}{\sqrt{\pi}}Q\partial_x\Phi(0) + \frac{P^2}{2m} + \frac{1}{2}m\omega_0^2 Q^2. \tag{5}$$

The bosonized Hamiltonian is identical to that of coupled harmonic oscillators.[28,29]

Due to the electron–phonon coupling g, the phonon mode softens as[18,29]

$$\omega_{p\pm} = -i\Gamma \pm \sqrt{\omega_0^2 - \Gamma^2 - \Gamma\omega_0^2/\Gamma_2}, \tag{6}$$

where $\Gamma_2 = \pi\omega_0^2/4W \ll \omega_0 \ll W$, W is the bandwidth of the conduction electrons, and $\Gamma = \pi(g\rho)^2/2m$ for small g, approaching Γ_2 as $g \to \infty$. Here, $\rho = 1/2\pi v_F$ is the chiral electron density of states. The explicit dependence of Γ on g cannot be determined by the bosonization approach.[29] The real part of the phonon frequency remains finite (underdamped) for $\Gamma < \Gamma_1 \approx \Gamma_2(1-\Gamma_2^2/\omega_0^2)$. For $\Gamma_1 < \Gamma < \Gamma_2$, the oscillatory behavior disappears from the phononic response (Re $\omega_{p\pm} = 0$) and two distinct dampings characterize it (overdamped). This softening is observable in many physical quantities, such as the enhancement of the local charge response, indicating the charge-Kondo phenomenon.

The local retarded Green's function of the conduction electrons is defined, using Eq. (2) as[30]

$$\begin{aligned} G_R(t) &= -i\Theta(t)\langle\{\Psi(x=0,t),\Psi^+(y=0,t=0)\}\rangle \\ &= -i\Theta(t)\frac{k_F^2}{4\pi}\sum_{\gamma,\gamma'=\pm}\lim_{\alpha\to 0}\langle\{R(\gamma\alpha,t),R^+(\gamma'\alpha,0)\}\rangle \\ &= -i\Theta(t)\frac{k_F^2}{8\pi^2}\sum_{\gamma,\gamma'=\pm}(\exp[C_{\gamma,\gamma'}(t)] \\ &\quad + \exp[C_{\gamma',\gamma}(-t)]), \end{aligned} \tag{7}$$

where $C_{\gamma,\gamma'}(t) = \lim_{\alpha\to 0} 4\pi\langle\Phi(\gamma\alpha,t)\Phi(\gamma'\alpha,0) - [\Phi(\gamma\alpha,t)^2 + \Phi(\gamma'\alpha,0)^2]/2\rangle - \ln(\alpha)$, whose second appearance in Eq. (7) follows from time-reversal symmetry, $\alpha \sim 1/W$ is the short-distance cutoff in the bosonized theory, and γ and γ' denotes the sign of the space coordinate. The impurity site is defined in terms of the chiral operators as the limiting value from Eq. (2). The $\gamma = \gamma'$ combinations do not contain any information about the presence of the impurity at the origin[31] since both field operators are taken on the same side of the impurity and no scattering is experienced. On the other hand, $\langle R(\gamma\alpha,t)R^+(-\gamma\alpha,0)\rangle$ describes scattering through the impurity and depends strongly on its properties. The expectation value $C_{\gamma,\gamma'}(t)$ at bosonic Matsubara frequencies can be evaluated from the bosonized Hamiltonian [Eq. (5)] as

$$C_{\gamma,\gamma'}(\omega_m) = -\frac{1}{4|\omega_m|} + \frac{\Gamma}{2}\frac{[\mathrm{sgn}(\omega_m)+\gamma][\mathrm{sgn}(\omega_m)-\gamma']}{(|\omega_m| + i\omega_{p+})(|\omega_m| + i\omega_{p-})}. \tag{8}$$

Then by analytical continuation to real frequencies, we can determine the spectral intensity following Ref. 32, which leads to the desired function, $C_{\gamma,\gamma'}(t)$. This follows the derivation of the position autocorrelator of a harmonic oscillator coupled to a heat bath.[28] The local retarded Green's function follows as

$$G_R(\omega) = -i\pi\frac{\rho_b}{2}\left(1 + F(\omega) + \left(\frac{\omega_{p+}}{\omega_{p-}}\right)^{4\Gamma i/(\omega_{p+}-\omega_{p-})}\right), \tag{9}$$

where

$$F(\omega) = \int_0^{\infty} dt\frac{\exp(i\omega t)}{\pi t}\mathrm{Im}\exp\left[\frac{4\Gamma(d[t\omega_{p+}] - d[t\omega_{p-}])}{i(\omega_{p+}-\omega_{p-})}\right], \tag{10}$$

and $d[x] = \exp(-ix)\{-\mathrm{Ci}(-x) + i[\mathrm{Si}(-x) - \frac{\pi}{2}]\}$ in the underdamped case, $\mathrm{Si}(x)$ and $\mathrm{Ci}(x)$ are the sine and cosine integrals, and $\rho_b = k_F^2/2\pi^2 v_F$ is the 3D bulk density of states. When Eq. (9) is expanded in Γ, it agrees with perturbative results.[33] We can identify the T matrix using the Dyson equation for the local Green's function as $G(0,\omega) = G_0(0,\omega) + G_0(0,\omega)T(\omega)G_0(0,\omega)$, where $G_0(0,\omega) = -i\pi\rho_b$ is the un-

perturbed Green's function. Therefore, we determine the full T matrix as

$$T(\omega) = \frac{i}{2\pi\rho_b}\left[\left(\frac{\omega_{p+}}{\omega_{p-}}\right)^{4\Gamma i/(\omega_{p+}-\omega_{p-})} + F(\omega) - 1\right], \quad (11)$$

which is the main result of this paper. It contains all the nonperturbative effects of the quantum impurity introduced in Eq. (1). As was shown in Ref. 5, this possesses all the information needed to evaluate the various cross sections. From this, we obtain the many-body s matrix as[34]

$$s(\omega) = 1 - i2\pi\rho_b T(\omega), \quad (12)$$

which stays always within the unit circle in the complex plane. The circumference of the unit circle denotes perfect elastic scattering. The total, elastic, and inelastic cross sections are readily evaluated from $s(\omega)$ as[5,6,34]

$$\sigma_{\text{tot}} = \frac{\sigma_0}{2}[1 - \text{Re } s(\omega)], \quad (13)$$

$$\sigma_{\text{inel}} = \frac{\sigma_0}{4}(1 - |s(\omega)|^2), \quad (14)$$

$$\sigma_{el} = \frac{\sigma_0}{4}(1 - 2\ \text{Re } s(\omega) + |s(\omega)|^2), \quad (15)$$

where $\sigma_0 = 2/\pi\rho_b v$ is the maximal value of the cross section. σ_{inel} is directly related to the dephasing time τ_ϕ, measured in weak-localization experiments.[5] A localized vibrational mode contributes to the inelastic-scattering rate even at $T=0$. The evolution of its s matrix is shown in Fig. 2. In the weak-coupling limit (small Γ), scattering is negligible. For small frequencies, the s matrix follows the upper semicircle, thus scattering is mostly elastic. For larger Γ, the weight of the inelastic component increases with Γ until it reaches its maximum value at $s=0$ at the critical coupling Γ_2. There, the total scattering cross section is divided equally between inelastic and elastic processes with weight $\sigma_0/4$ for $|\omega_{p\pm}| \ll \omega \ll W$, similarly to the channel isotropic two-channel Kondo model at $\omega=0$, which is a prototype model for non-Fermi-liquid behavior. However, the classification of impurity states as Fermi or non-Fermi-liquid becomes inappropriate in the present case since scattering is caused by bosonic, and not fermionic, modes. Since the transition occurs at $g \to \infty$ ($\Gamma \to \Gamma_2$), the crossing of this critical point is impossible.

Figure 3 shows the total, elastic-, and inelastic-scattering rates as a function of frequency for several Γ. At zero frequency, all rates vanish since the electron Green's function is pinned to its noninteracting value due to some generalized Fermi-liquid relations;[2,16] therefore $\sigma_{\text{tot,inel},el}=0$ at $\omega=T=0$. For small couplings and $\omega < \text{Re } \omega_{p\pm}$, the ground state contains no phonons but a filled Fermi sea; thus electrons scatter off elastically. By exceeding this threshold (Re $\omega_{p\pm}$), the total scattering is mainly given by the inelastic cross section, which develops steps at $n \times |\omega_{p\pm}|$ (with n integer), stemming from n-phonon excitations. At $n=1$, this is also predicted by perturbation theory[33] as $\sigma_{\text{tot}} \approx \sigma_{\text{inel}} = \sigma_0 \Gamma \pi \Theta(\omega - \omega_0)/\omega_0$. Higher steps occur with smaller weight in alternating fashion. At the same time, the elastic rate exhibits a small cusp at ω_0 due to the logarithmic singularity of the real part of electron self energy.[33]

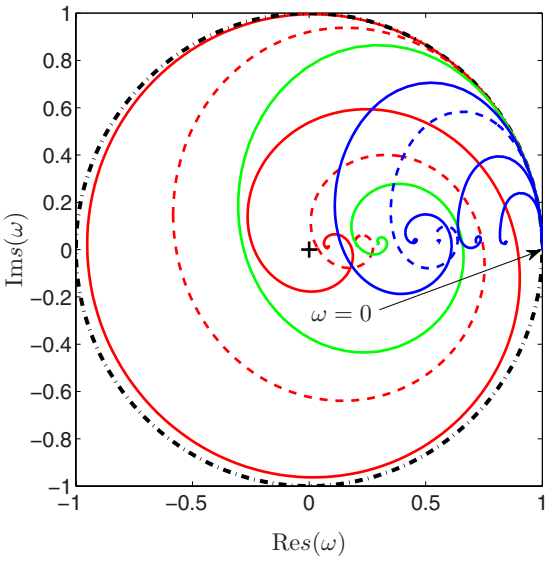

FIG. 2. (Color online) The evolution of the s matrix on the complex plane is shown at $T=0$ for $W=10\omega_0$, $\Gamma/\Gamma_2=0.3$, 0.5, 0.7 (blue dashed line), 0.8 (blue lines), 0.9 (green line), 0.94 (red dashed line), and 0.98 (red solid line) from right to left. Close to the critical coupling $\Gamma=\Gamma_2$, the scattering is dominantly elastic for small frequencies and follows the unit circle. Then, it reaches rapidly the maximal inelastic rate ($s=0$) with increasing ω because at the critical coupling the phonon excitation energy $|\omega_{p-}| \to 0$, facilitating inelastic processes.

For larger couplings, these sharp steps become smeared and turn into oscillations due to the finite lifetime of the phonons. These oscillations are not of Friedel type, corresponding to the interference of incoming and scattered waves, but arise from multiphonon excitations. The elastic-scattering rate grows progressively and becomes the dominant scattering mechanism for one and two phonon excitations. By approaching the critical coupling Γ_2, the inelastic scattering reaches its maximum since the vanishing phonon energy, ω_{p-}, makes arbitrary multiphonon processes possible. In two experiments on artificial quantum dots,[9,10] the renormalized phonon frequency fell into the 0.5–50 K range. In general, the renormalization of the bare phonon frequency (ω_0) depends strongly on the phonon mass m and the coupling to the electrons g, as is shown in Eq. (6), and the resulting $\omega_{p\pm}$ can take practically any value below ω_0. These results at $T=0$ are in marked contrast to those found for Kondo impurities.[5–7]

In actual experiments (on, e.g., Ag or Au samples with Fe impurities), the dephasing time is measured at finite temperatures and can be decomposed as $1/\tau_\phi = 1/\tau_{e-e} + 1/\tau_{e\text{-ph}} + 1/\tau_{\text{imp}}$. In the high-temperature limit, it is dominated by the bulk electron–electron ($1/\tau_{e-e} \sim T^{2/3}$) and electron–phonon ($1/\tau_{e\text{-ph}} \sim T^3$) interactions, and is accounted for by the Altshuler-Aronov-Khmelnitzky theory.[35] At lower temperatures, the impurity contribution becomes important ($1/\tau_{\text{imp}} \sim n_{\text{imp}}\sigma_{\text{inel}}$) and scales with the impurity concentration n_{imp}. Magnetic impurities account successfully for this latest con-

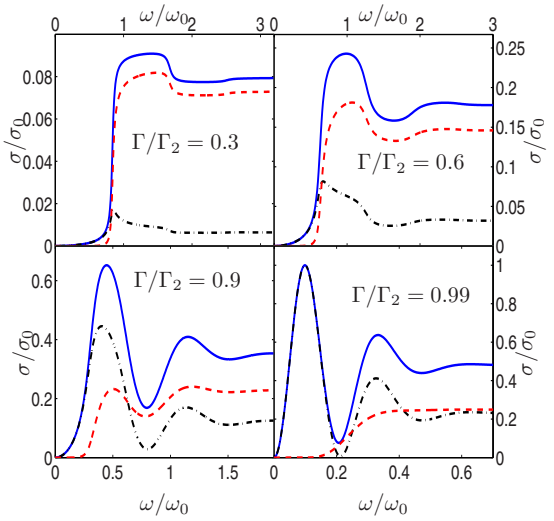

FIG. 3. (Color online) The frequency dependent scattering cross sections are shown for $W=10\omega_0$, $\Gamma/\Gamma_2=0.3$, 0.6, 0.9, and 0.99 from left to right and top to bottom. The solid blue, red dashed, and black dashed-dotted lines denote $\sigma_{\rm tot}$, $\sigma_{\rm inel}$, and σ_{el}, respectively. For small frequencies, all scattering rates vanish. Then, wild oscillations show up, representing the various multiphonon (n-phonon) processes, setting in at $n\times|\omega_{p\pm}|$. At higher frequencies ($|\omega_{p\pm}|\ll\omega\ll W$), inelastic processes dominate. With increasing Γ, the weights of both elastic and inelastic processes increase. By approaching the critical coupling, the inelastic-scattering rate reaches its maximal value, $\sigma_0/4$, because with the vanishing phonon frequency, ω_{p-}, phonon excitations become more likely, favoring inelastic scatterings. Note the different horizontal and vertical scales on the figures.

tribution down to $0.1T_K$ (with T_K the Kondo temperature).[3,4]

Our calculation on the local oscillator model can be extended to finite temperatures. Conformal invariance can only be used for times much bigger[27] than $1/\omega_0$, which translates to $T\ll\omega_0$, leading to T^2 corrections to the scattering rates at $(T,\omega)\ll\omega_0$. Note that all scattering rates at $T=\omega=0$ vanish. The same conclusion was born out from the generalized Fermi-liquid relations.[2,16] In the 4 Re $\omega_{p\pm}\lesssim T\ll W$ range, the inelastic-scattering rate reaches its maximal value, $\sigma_{\rm inel}=\sigma_{el}=\sigma_0/4$, since at high temperatures the phonon state is highly populated, facilitating inelastic scattering. This behavior is similar to the $T=0$ case close to the softening $\Gamma\to\Gamma_2$, where the vanishing phonon excitation frequency favors inelastic processes. In between these two regions ($T\sim\omega_0$), a smooth crossover takes place.

The Kondo picture starts to deviate from the experimental data below the Kondo temperature.[7,36,37] This mismatch is cured by introducing a very small amount of magnetic impurities with a very low Kondo temperature[7] or by adding a constant background.[37] Instead, a flat, temperature-independent dephasing time (with $\omega_0\ll 0.1T_K\ll W$) follows naturally from local vibrational modes, originating from the implantation process, as was demonstrated above, and serves as an obvious explanation for the measured behavior. Therefore, local vibrational modes can account successively for the measured dephasing time in weak-localization experiments. The second crucial difference with respect to Kondo impurities arises from the magnetic-field insensitivity of the phonons, and requires further experiments to reveal the differences.[14]

In conclusion, we have demonstrated through an exact solution of the single impurity Holstein or Yu-Anderson model that local vibrational modes can have a strong impact on the dephasing time of electrons. The inelastic-scattering rate exhibits strong oscillations at frequencies comparable to the phonon excitation energy and then saturates to a finite, coupling dependent value. At the extreme strong-coupling limit, close to the complete softening of the phonons, the s matrix vanishes and the inelastic cross section reaches its maximal value. This phonon mediated scattering mechanism is expected to be rather insensitive to the applied magnetic field, in contrast to Kondo-type impurities, and can contribute to the dephasing time in certain alloys containing dynamical defects.[9,14]

Useful and illuminating discussions with Peter Fulde and Sergej Flach are gratefully acknowledged. This work was supported by the Hungarian Scientific Research Fund under Grant No. K72613.

*dora@pks.mpg.de

[1] P. Mohanty, E. M. Q. Jariwala, and R. A. Webb, Phys. Rev. Lett. **78**, 3366 (1997).
[2] A. C. Hewson, *The Kondo Problem to Heavy Fermions* (Cambridge University Press, Cambridge, 1993).
[3] G. Zaránd, L. Borda, J. von Delft, and N. Andrei, Phys. Rev. Lett. **93**, 107204 (2004).
[4] T. Micklitz, A. Altland, T. A. Costi, and A. Rosch, Phys. Rev. Lett. **96**, 226601 (2006).
[5] L. Borda, L. Fritz, N. Andrei, and G. Zaránd, Phys. Rev. B **75**, 235112 (2007).
[6] T. Micklitz, T. A. Costi, and A. Rosch, Phys. Rev. B **75**, 054406 (2007).
[7] C. Bäuerle, F. Mallet, F. Schopfer, D. Mailly, G. Eska, and L. Saminadayar, Phys. Rev. Lett. **95**, 266805 (2005).
[8] M. Galperin, M. A. Ratner, and A. Nitzan, J. Phys.: Condens. Matter **19**, 103201 (2007).
[9] H. Park, J. Park, A. K. L. Lim, E. H. Anderson, A. P. Alivisatos, and P. L. McEuen, Nature (London) **407**, 57 (2000).
[10] E. M. Weig, R. H. Blick, T. Brandes, J. Kirschbaum, W. Wegscheider, M. Bichler, and J. P. Kotthaus, Phys. Rev. Lett. **92**, 046804 (2004).
[11] S. Sanada, Y. Aoki, H. Aoki, A. Tsuchiya, D. Kikuchi, H. Sugawara, and H. Sato, J. Phys. Soc. Jpn. **74**, 246 (2005).
[12] S. Yotsuhashi, M. Kojima, H. Kusunose, and K. Miyake, J. Phys. Soc. Jpn. **74**, 49 (2005).
[13] T. Hotta, J. Phys. Soc. Jpn. **76**, 023705 (2007).
[14] S. M. Huang, T. C. Lee, H. Akimoto, K. Kono, and J. J. Lin, Phys. Rev. Lett. **99**, 046601 (2007).
[15] J. Fransson and A. V. Balatsky, Phys. Rev. B **75**, 195337 (2007).

[16] P. S. Cornaglia, D. R. Grempel, and H. Ness, Phys. Rev. B **71**, 075320 (2005).
[17] N. F. Schwabe, A. N. Cleland, M. C. Cross, and M. L. Roukes, Phys. Rev. B **52**, 12911 (1995).
[18] J. W. Gadzuk, Phys. Rev. B **24**, 1651 (1981).
[19] C. C. Yu and P. W. Anderson, Phys. Rev. B **29**, 6165 (1984).
[20] V. Y. Irkhin and M. I. Katsnelson, Fiz. Tverd. Tela (S.-Peterburg) **28**, 3648 (1986).
[21] E. W. Montroll and R. B. Potts, Phys. Rev. **100**, 525 (1955).
[22] M. I. Molina, J. A. Rössler, and G. P. Tsironis, Phys. Lett. A **234**, 59 (1997).
[23] A. C. Hewson and D. Meyer, J. Phys.: Condens. Matter **14**, 427 (2002).
[24] P. S. Cornaglia, H. Ness, and D. R. Grempel, Phys. Rev. Lett. **93**, 147201 (2004).
[25] A. Zawadowski, J. von Delft, and D. C. Ralph, Phys. Rev. Lett. **83**, 2632 (1999).
[26] Y. Imry, H. Fukuyama, and P. Schwab, Europhys. Lett. **47**, 608 (1999).
[27] A. O. Gogolin, A. A. Nersesyan, and A. M. Tsvelik, *Bosonization and Strongly Correlated Systems* (Cambridge University Press, Cambridge, 1998).
[28] U. Weiss, *Quantum Dissipative Systems* (World Scientific, Singapore, 2000).
[29] B. Dóra, Phys. Rev. B **75**, 245113 (2007).
[30] P. Kakashvili, H. Johannesson, and S. Eggert, Phys. Rev. B **74**, 085114 (2006).
[31] M. Fuentes, A. Lopez, E. Fradkin, and E. Moreno, Nucl. Phys. B **450**, 603 (1995).
[32] D. N. Zubarev, Sov. Phys. Usp. **3**, 320 (1960).
[33] S. Engelsberg and J. R. Schrieffer, Phys. Rev. **131**, 993 (1963).
[34] D. C. Langreth, Phys. Rev. **150**, 516 (1966).
[35] B. L. Altshuler, A. G. Aronov, and D. E. Khmelnitzky, J. Phys. C **15**, 1497 (1982).
[36] G. M. Alzoubi and N. O. Birge, Phys. Rev. Lett. **97**, 226803 (2006).
[37] F. Mallet, J. Ericsson, D. Mailly, S. Ünlübayir, D. Reuter, A. Melnikov, A. D. Wieck, T. Micklitz, A. Rosch, T. A. Costi, L. Saminadayar, and C. Bäuerle, Phys. Rev. Lett. **97**, 226804 (2006).